CRYSTAL GROWTH & DESIGN

Article

pubs.acs.org/crystal

Suppressed Crystallization of Rod-Disc Molecule by Surface Anchoring Confinement

Dae-Yoon Kim,[#,†] Prasenjit Nayek,[#,†] Soeun Kim,[†] Kyung Su Ha,[†] Mi Hyeon Jo,[†] Chih-Hao Hsu,[‡] Yan Cao,[‡] Stephen Z. D. Cheng,[‡] Seung Hee Lee,*[,†] and Kwang-Un Jeong*[,†]

[†]Polymer Materials Fusion Research Center, Department of Polymer-Nano Science and Technology, Department of Flexible and Printable Electronics, and Department of BIN Fusion Technology, Chonbuk National University, Jeonju, 561-756, Korea

[‡]College of Polymer Science and Engineering, The University of Akron, Akron, Ohio 44325, United States

ABSTRACT: Upon varying the thickness of liquid crystal (LC) cells and alternating their surface chemical and physical environments, phase transition behaviors of the rod-disc molecule (RD12, where 12 is the number of carbon atoms in each alkyl chain linkage between the rod and the disc mesogens) were dramatically changed. From the cross-polarized optical microscopic observations and analyses, it was realized that the macroscopically oriented nematic (N) phase of RD12 was obtained by the surface anchoring confinement and the crystallization of RD12 was completely suppressed. On the basis of the systematic experimental investigations, it was concluded that the glassy N phase was formed because the interaction between surface alignment layer and RD12 (a surface anchoring force) is bigger than that of RD12 themselves (a driving force of the crystallization). The finely tuned molecular orientations and anisotropic physical properties of the programmed RD12 building compound can allow us to fabricate smart optical and electrical thin films for practical applications in electro-optical applications.

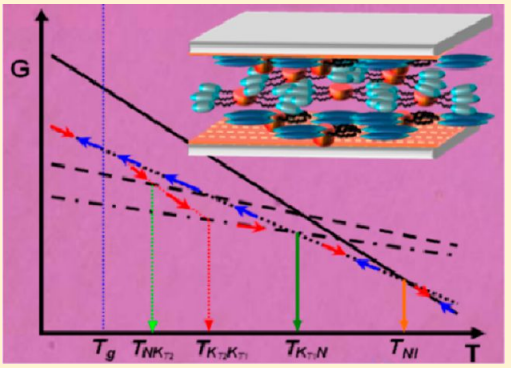

INTRODUCTION

Since the first discovery of liquid crystal (LC) in the 1880s by Reinitzer and Lehmann, novel LC molecules have been designed, synthesized, and characterized not only for better understanding of mesophase concepts in soft materials as an important basic scientific aspect but also for the innovation of new technologies, especially in LC displays (LCDs).[1−19] In scientific aspects, these novel LC molecules have introduced unique ordered phases, such as twist grain boundary phases,[20−22] blue phases,[23−25] achiral banana phases,[26−30] and biaxial nematic (N) LC phases.[31−33] The newly introduced LC molecules have, on the other hand, encouraged engineers to fabricate the various types of LCDs which are ubiquitous displays in televisions, computers, mobile phones, and navigators.[34−36]

From this perspective, we have reported the characteristics of the rod-disc molecule (RD12), which was newly synthesized by the chemical combination of rodlike (R) and disclike (D) mesogens.[37−40] The chemical structure of RD12 is illustrated in Figure 1. Through combined experimental results and careful analyses, it was realized that the RD12 molecule can form three different ordered phases by decreasing the temperature from the isotropic (I) phase: N phase, stable K_{T1} crystalline phase, and metastable K_{T2} crystalline phase.[37−40] Utilizing the two-dimensional X-ray diffraction technique, the biaxial N molecular arrangement of RD12 was demonstrated under a direct current (DC) electric field.[37−40] Upon varying the alternating current (AC) electric fields, molecular orientation of RD12 was

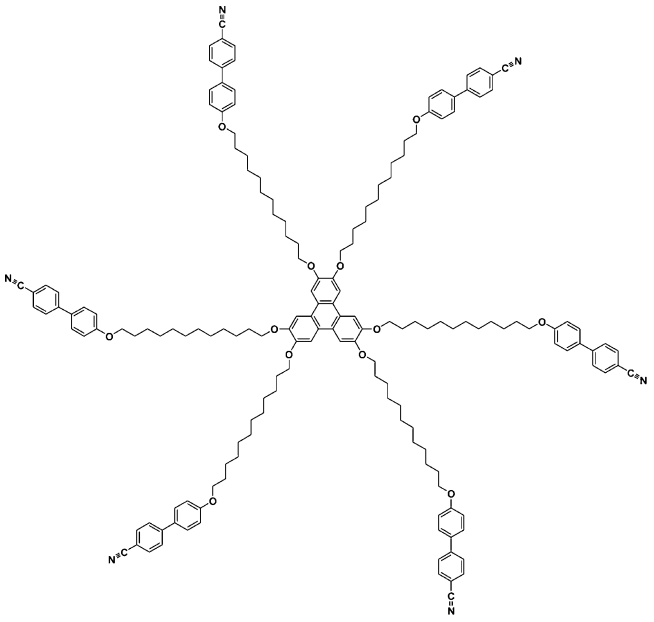

Figure 1. Chemical structure of rod-disc molecule (RD12).

Received: December 3, 2012
Revised: January 18, 2013
Published: January 30, 2013

systematically investigated in the vertical as well as in-plane electric fields.[41] Surprisingly, RD12 responded to the electric field with a two-step process in the vertical electric field LC cell. After frustration and stabilization of the rod mesogens, the whole RD12 molecule was aligned parallel to the vertically applied electric field.[41] It was also found that the molecular frustrations of RD12 under the vertical AC electric field as a result of the competition between the rod mesogens attached to both sides of the disc mesogen. Furthermore, since the birefringence (Δn = 0.172 at 122.7 °C) of optical RD12 films can be controlled by magnetic and/or electric fields, tunable optical switches may be fabricated.[37−41]

Although RD12 molecular orientational behaviors under electric fields with alignment layers have been clearly understood, the phase transition behaviors in the confined LC cell with a planar alignment layer have not yet been revealed. In this research, we have observed that the N phase of RD12 is effectively preserved and does not transfer to the stable K_{T1} crystalline phase even though the LC cell with a planar alignment layer (rubbed polyimide, PI) and a typical cell thickness (d = 4.4 μm) can be cooled to below the glass transition temperature (T_g = 38 °C) of RD12. A question is still remaining: what is the cause of the disappearance of the N → K_{T1} phase transition in this LC cell? To find the possible reasons for this question, phase transition behaviors of RD12 in the LC cells have been investigated upon varying the LC cell thicknesses and alternating the surface chemistry and physics. On the basis of our experimental observations and analysis, we found that the temperature range of this N LC phase of RD12 in the LC cell with a low cell thickness and PI rubbed surface can be expanded, and the crystallization has been completely suppressed. The formation of the glassy N phase may be because the interaction between the surface PI alignment layer and RD12 is bigger than that of RD12 molecules themselves.

EXPERIMENTAL SECTION

Rod-disc LC molecules (RD12) were synthesized by four-step condensation reactions.[37−40] The chemical structure of RD12 purified by chromatography on silica gel using chloroform/hexane (6/1) mixed solvent as an eluent was verified by thin-layer chromatography, MALDI-TOF mass spectrometry, elemental analysis, and proton nuclear magnetic resonance spectroscopy (^{1}H NMR).[37−40] The Cerius^2 (Version 4.6, Accelrys) simulation software with the COMPASS force field was applied to estimate the energy minimized geometry of RD12 in the isolated gas-phase.[37−40] The calculated diameter of the triphenyl discotic core was 1.02 nm, and the length of each cyanobiphenyl rod was 2.65 nm.[37−40] When the alkyl chains between six rods and one disc were assumed to be in the all-trans conformation, the diameter of RD12 molecular disc was calculated to be 6.32 nm.[37−40]

To study the crystallization behavior of RD12 by varying the thickness of the LC cells and alternating their surface chemical and physical environments, the antiparallel-rubbed electro-optic LC cells were fabricated with a planar alignment layer (Japan Synthetic Rubber, AL-16139, Japan) coated on indium tin oxide (ITO) glass substrates, as schematically illustrated in Figure 2a. This type of LC cell is named as electrically controlled birefringence (ECB) cell.[42−44] Applying a spin coater (Korea Spin Coater system, ECF-2, Korea), a planar alignment layer polyimide (PI) was first coated on ITO glass substrates. The spinning rate was increased up to 2800 rpm and maintained for 70 s after spin coating at 550 rpm for 20 s. The spin-coated substrates were cured in a drying oven (JEIO TECH, NO-600M, Korea) with a two-step process: curing first at 80 °C for 5 min and then at 180 °C for 1 h. The post curing process at 180 °C was conducted for securing the adhesion between ITO glass substrate and alignment layer. The thickness of cured planar alignment layers was

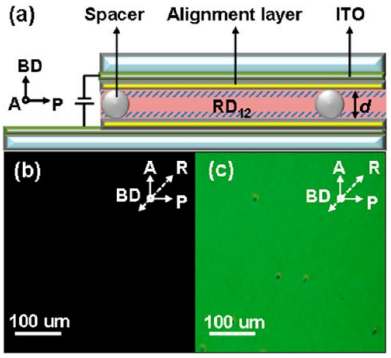

Figure 2. (a) Schematic illustration of the RD12-filled LC cell and POM images when the rubbing direction (R) is arranged to be 45° with respect to the axes of A and P in the (b) I and (c) N phases.

controlled to be 100 nm. After the antiparallel rubbing process, two substrates were assembled into a sandwich LC cell by utilizing an automatic press (Neo system, APD-01, Japan). Plastic ball spacers with a diameter of about 4.4, 9.0, or 20 μm were purposely added between the substrates in order to maintain the uniform cell thickness (d). Using a cell thickness measurement (Sesim Photonics Technology, CGMS-100T, Korea), the cell thickness was experimentally determined. Utilizing osmotic pressure, RD12 was injected into the fabricated LC cell. Polarizer (P) and analyzer (A) were arranged perpendicular to each other, and the antiparallel rubbing direction (S) of substrate was set to be 45° with respect to P and A for clear morphological observations.

Phase transition behaviors of the RD12-filled LC cell were investigated by texture observations using cross-polarized optical microscopy (POM, Nikon, Eclipse E650 POL, Japan) equipped with a temperature controller (Linkam, TMS94, UK). To remove the prehistoric effects of RD12, the RD12-filled LC cell was first heated to above 145 °C and left for 5 min and then cooled down to a certain temperature at 1 °C/min. Contact angles of the LC substrates were measured with a contact angle measurement instrument (CAM-WAFER, Tantec Inc., USA).[45−47]

RESULTS AND DISCUSSION

Phase Behaviors of RD12 Molecule in the Bulk State.

Rod-disc LC molecule (RD12) schematically illustrated in Figure 1 exhibits three ordered phases below the isotropization temperature (T_{NI} = 130 °C) in the bulk RD12. The N LC phase arises first at 130 °C during the cooling process, and the

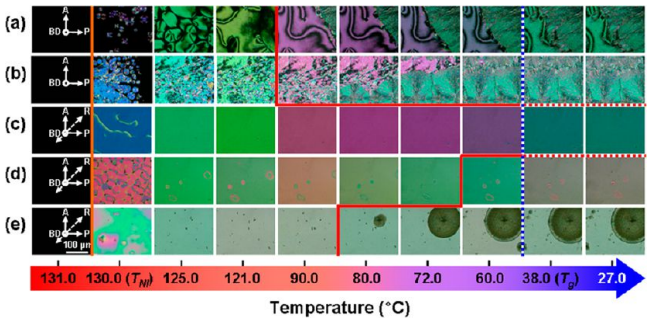

Figure 3. POM images of the RD12-filled LC cell taken at different temperatures by cooling at 1 °C/min: (a) pristine ITO LC cell with d = 4.4 μm, (b) PI coated LC cell with d = 4.4 μm, (c) PI coated/rubbed LC cell with d = 4.4 μm, (d) PI coated/rubbed LC cell with d = 9.0 μm, and (e) PI coated/rubbed LC cell with d = 20 μm. The orange and red solid lines stand for the transitions of I → N and N → K_{T1}, respectively. The blue solid line represents the T_g = 38 °C of RD12 and the POM image in the dotted box indicates the glassy N phase.

dx.doi.org/10.1021/cg301777y | Cryst. Growth Des. 2013, 13, 1309−1315

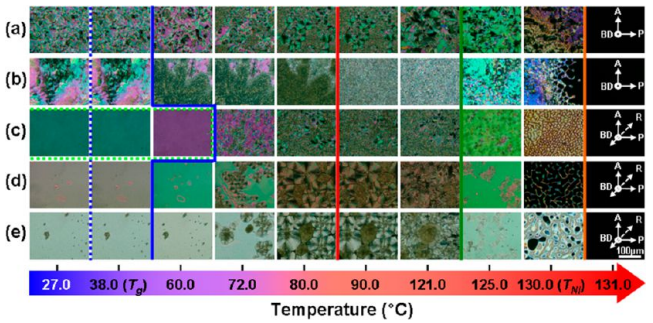

Figure 4. POM images of the RD12-filled LC cell taken at different temperatures by a heating process at 1 °C/min right after quenching the LC cell below T_g = 38 °C: (a) pristine ITO LC cell with d = 4.4 μm, (b) PI coated LC cell with d = 4.4 μm, (c) PI coated/rubbed LC cell with d = 4.4 μm, (d) PI coated/rubbed LC cell with d = 9.0 μm, and (e) PI coated/rubbed LC cell with d = 20 μm. Here, the blue solid line represents the T_g = 38 °C of RD12, and above this temperature the metastable K_{T2} phase gradually emerged in panel c. The red and green solid lines stand for $K_{T2} \rightarrow K_{T1}$ and $K_{T1} \rightarrow$ N transitions, respectively. The orange solid line corresponds to the transition of N → I, and the POM image in the dotted line box indicates the glassy N phase.

stable K_{T1} and the metastable K_{T2} crystalline phases are also formed below the N LC phase. Here, the metastable K_{T2} crystalline phase is formed at 72 °C during a subsequent heating process after cooling RD12 below the glass transition temperature (T_g = 38 °C). The metastability of K_{T2} crystalline phase is confirmed by the observation of the $K_{T2} \rightarrow K_{T1}$ transition by the isothermal annealing and the heating processes as well as the spherulitic morphological investigation of these two triclinic crystals.[37−40] The phase transition behaviors of RD12 molecule in the bulk can be manipulated by the introduction of external forces, such as a surface anchoring interaction.[41,48−54]

Phase Behaviors of RD12 Molecule Manipulated by Surface Anchoring Interactions. To test this speculation, the surface chemistry of LC cell substrates and the physical interactions between RD12 molecule and surface of substrates are tuned by coating and rubbing the PI alignment layers. Additionally, the LC cell thickness is controlled in the range of 4.4−20 μm to investigate the competition between the surface anchoring interaction (between the surface PI alignment layer and RD12 molecules) and the driving force of crystallization (among RD12 molecules in the bulk). The fabricated RD12-filled LC cell is schematically illustrated in Figure 2a. Here, the axes of polarizer (P) and analyzer (A) are arranged perpendicular to each other, and the rubbing direction (R) of antiparallelly arranged LC cell is set to be 45° with respect to P and A for the clear morphological observations, as indicated in Figure 2.

To confirm the macroscopic RD12 arrangement in the N LC phase due to the surface anchoring forces between RD12 and the planar alignment layers, the RD12-filled LC cell with the PI coated/rubbed planar alignment layer and d = 4.4 μm is first heated to its I phase and then gradually cooled to below T_{NI} = 130 °C. As expected, the POM image in the I phase is completely dark (Figure 2b). In the N phase, the cell exhibits some transmittance when the R is arranged to be 45° from the transmission axes of crossed polarizers (Figure 2c). On the other hand, a complete dark state is obtained again when the cell is rotated 45° to be parallel to the A or P axes. From these POM experimental observations, it is revealed that the optical axis of RD12 is macroscopically and uniformly oriented along the R. By introducing the PI rubbed alignment layer, the long axes of the rod and the in-plane axis of the disc mesogens in RD12 are aligned parallel to the R due to the surface anchoring interactions between RD12 and the alignment layers. Note that the overall shape of RD12 in the cell (d = 4.4 μm) with the rubbed alignment layers must be ribbonlike rather than disclike. The retardation value of RD12 cell (0.762 μm) obtained by comparing with colors in the Michel-Lévy birefringence chart provides a clear explanation of the greenish color in the POM image of the RD12-filled cell (Figure 2c).[55]

Even though the LC cell is cooled at a slow cooling rate (1 °C/min) to below the T_g of RD12, the N phase of RD12 is effectively preserved and does not transfer to the K_{T1} or K_{T2} crystalline phases. Namely, the temperature region where the N phase appears is greatly expanded. To find the plausible reasons for the disappearance of this N → K_{T1} phase transition in the LC cell, phase transition behaviors of RD12 in the LC cells with

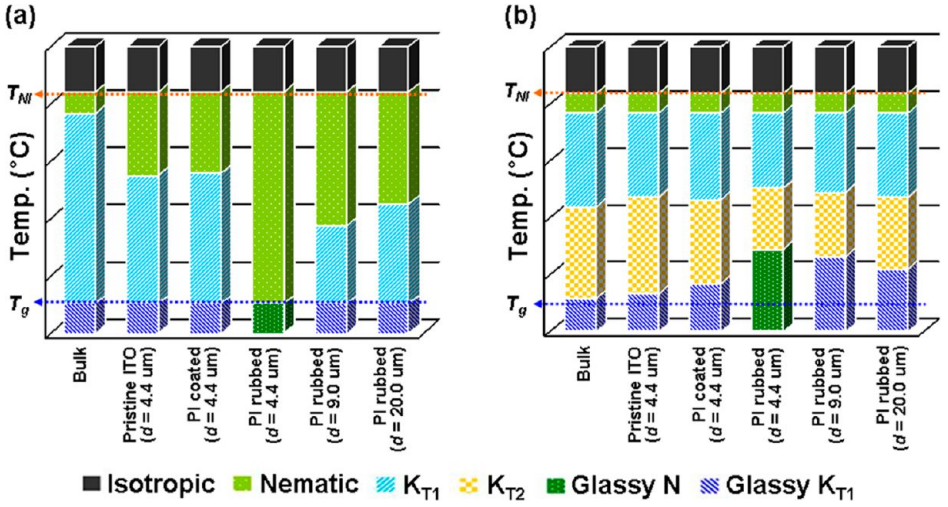

Figure 5. Phase transition diagrams of RD12 were constructed based on the POM morphological observations during the (a) cooling and (b) subsequent heating processes at a rate of 1 °C/min.

dx.doi.org/10.1021/cg301777y | Cryst. Growth Des. 2013, 13, 1309−1315

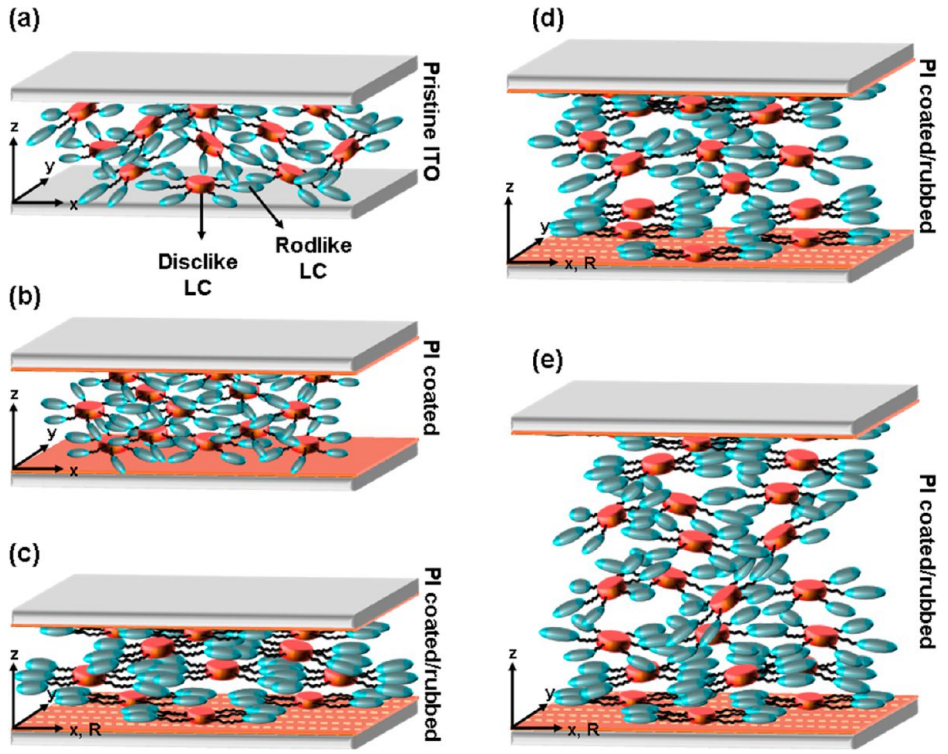

Figure 6. Schematic illustrations of RD12 molecular orientation in the RD12-filled LC cells: (a) pristine ITO LC cell with d = 4.4 μm, (b) PI coated LC cell with d = 4.4 μm, (c) PI coated/rubbed LC cell with d = 4.4 μm, (d) PI coated/rubbed LC cell with d = 9.0 μm, and (e) PI coated/rubbed LC cell with d = 20 μm.

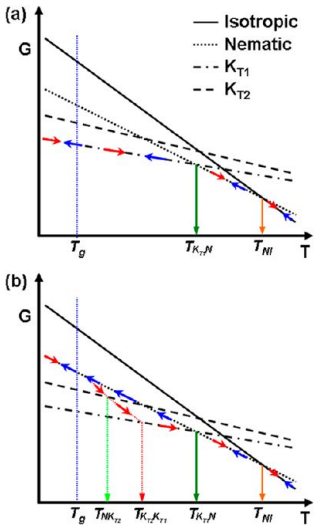

Figure 7. Illustration of the free energy versus temperature at constant pressure: (a) RD12 bulk sample and (b) RD12-filled PI coated/rubbed LC cell with d = 4.4 μm. Here, blue and red arrows represent the cooling and heating tracks.

varying the cell thicknesses and alternating the surface chemistry and physical environments are investigated.

When the pristine LC cell (d = 4.4 μm) without an alignment layer is cooled from the I phase at 1 °C/min (Figure 3a), the T_{NI} is identical to that of the bulk RD12. The N → K_{T1} phase transition is detected, but its transition temperature (T_{NKT1}) is shifted from 121 to 94 °C compared with that of the bulk RD12. The T_{NKT1} shift can be due to the surface chemistry of the substrates and/or the LC cell thickness. To identify the origin of T_{NKT1} shift, PI coated LC cell is prepared with an identical cell thickness (d = 4.4 μm). It is found that both T_{NI} (130 °C) and T_{NKT1} (96 °C) of the PI coated LC cell are similar to those of the pristine LC cell. The physical interaction between RD12 and LC cell substrates is estimated from the contact angles with deionized water and diiodomethane. Since the contact angles of pristine ITO (88° with deionized water and 40° with diiodomethane) and PI coated substrates (80° with deionized water and 34° with diiodomethane) are not much different, it is projected that the physical interactions between RD12 and LC cell substrates are little affected by the PI coating. These experimental results indicate that the T_{NKT1} shift from 121 (bulk) to 94 °C (pristine LC cell with d = 4.4 μm) is mainly due to the decrease of the LC cell thickness. The d-reduction results in the physical interaction enhancement between the surface PI alignment layer and RD12 molecules relative to that of RD12 themselves.

This result makes us conjecture that the N → K_{T1} phase transition can be completely suppressed by increasing the surface anchoring interactions between RD12 and substrates and by decreasing the cell thickness. It is well-known that the surface anchoring interactions between the LC molecule and substrate can be significantly enhanced by the PI coating/rubbing processes. The contact angles of the PI coated/rubbed substrates with deionized water and diiodomethane are measured to be 100° and 48°, respectively. To test the speculation, the PI coated/rubbed LC cell is prepared with an equal cell thickness (d = 4.4 μm). Upon cooling the PI coated/rubbed LC cell at 1 °C/min, the T_{NI} is identical to that of the bulk RD12. The N → K_{T1} phase transition completely disappeared and the temperature range of this N phase can be expanded, as shown in Figure 3c. From the phase transition behaviors of pristine LC cell (Figure 3a), PI coated LC cell (Figure 3b) and PI coated/rubbed LC cell (Figure 3c)

dx.doi.org/10.1021/cg301777y | Cryst. Growth Des. 2013, 13, 1309−1315

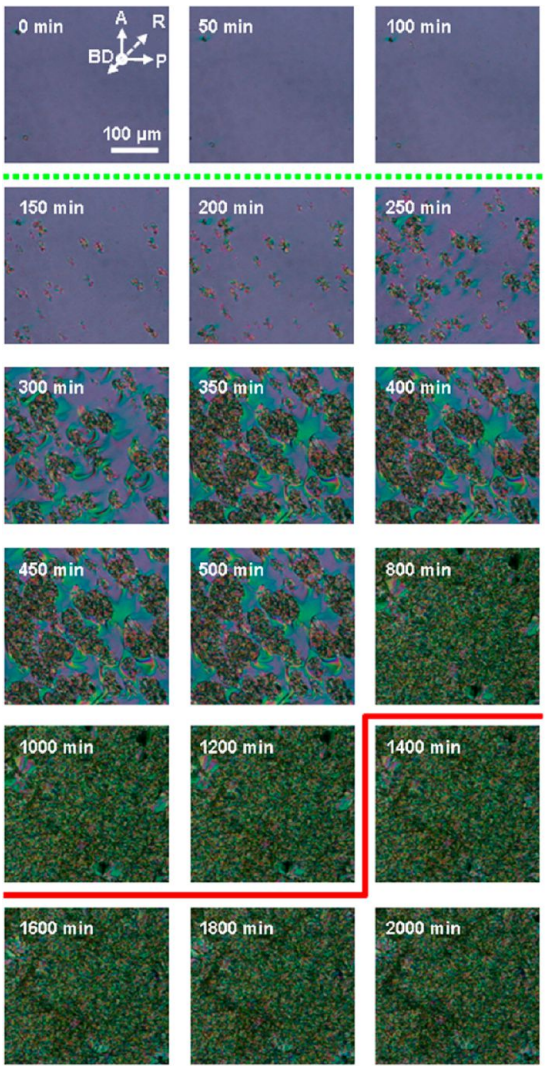

Figure 8. POM images of the RD12-filled PI coated and rubbed LC cell with d = 4.4 μm taken at different annealing times at 50 °C. Note that the annealing temperature is above the T_g = 38 °C. Red line stands for the $K_{T2} \rightarrow K_{T1}$ phase transition.

compared with those of the bulk RD12, it is clear that there are three factors to depress the N → K_{T1} phase transition: cell thickness (d), surface chemistry (PI coating), and physical interactions (PI coating/rubbing).

A series of PI coated/rubbed LC cells are fabricated with respect to the LC cell thickness to monitor the T_{NKT1} shift. At a cooling rate of 1 °C/min, PI coated/rubbed LC cells with d = 9.0 μm (Figure 3d) and d = 20.0 μm (Figure 3e) exhibit the T_{NI} at 130 °C. Note that the T_{NI} is independent of the surface chemistry and physics and the cell thickness. As shown in Figure 3d,e, the T_{NKT1} of the PI coated/rubbed LC cells with d = 9.0 μm (Figure 3d) and d = 20.0 μm (Figure 3e) is detected at 72 and 81 °C, respectively. As expected, T_{NKT1} increases with the cell thickness. With a simple linear assumption between the cell thickness and T_{NKT1} in this system, the surface anchoring interactions between RD12 molecules and the PI coated/rubbed LC substrates can be ignored when the cell thickness is above d = 68 μm.

Upon heating the LC cells at 1 °C/min right after the cooling process, the glassy N phase jammed below the T_g (38 °C) transfers to the K_{T2} crystalline mesophase at 40 °C (bulk), 42 °C (pristine LC cell with d = 4.4 μm), 46 °C (PI coated LC cell with d = 4.4 μm), 61 °C (PI coated/rubbed LC cell with d = 4.4 μm), 58 °C (PI coated/rubbed LC cell with d = 9.0 μm), and 53 °C (PI coated/rubbed LC cell with d = 4.4 μm). From these results, it is evident that the T_{NKT2} increases with the surface anchoring interaction between RD12 molecule and cell substrate and decreases with increasing the cell thickness. This reflects that a higher thermal energy is required for RD12 to overcome an energy barrier to enter a lower free energy state (K_{T2}) when the surface anchoring interaction increases and/or the cell thickness decreases. Note that below the T_g, the cooperative translational motions of RD12 are frozen, and all the LC cells do not transfer to any crystalline states. The POM observations reveal that the LC morphologies below the T_g are not changed at least for three months. The continuous heating process evolves the $K_{T2} \rightarrow K_{T1}$ phase transitions at 80 °C (bulk), 83 °C (pristine LC cell with d = 4.4 μm), 83 °C (PI coated LC cell with d = 4.4 μm), 88 °C (PI coated/rubbed LC cell with d = 4.4 μm), 86 °C (PI coated/rubbed LC cell with d = 9.0 μm), and 84 °C (PI coated/rubbed LC cell with d = 4.4 μm). These results indicate that the $K_{T2} \rightarrow K_{T1}$ phase transition temperature of the LC cell is little affected by the surface chemistry and physics and the cell thickness. As shown in Figure 4, the K_{T1} → N and N → I phase transition temperatures of the LC cells are identical with those in the bulk RD12. On the basis of these experimental results, it is concluded that after the complete transformation from the metastable K_{T1} crystalline phase to the stable K_{T1} phase, the thermodynamic phase transitions are independent of the surface anchoring interaction. The phase transition behaviors during the cooling and the subsequent heating at 1 °C/min are also summarized in Figure 5, panels a and b, respectively.

Both effects of the cell thickness and the planar alignment surface layer for RD12 on the phase transition behavior can be explained by schematic illustrations, as shown in Figure 6. Without the PI coating/rubbing process, RD12 below the T_{NI} does not form the uniform monodomain (Figures 3a,b and 6a,b). It is considered that both rod and disc mesogens directly contacting to the substrates are lying down (a phase-on arrangement) due to the physical interactions between RD12 mesogens and substrates. The whole shape of RD12 thus maintains a disclike shape. Getting away from the surface, RD12 gradually becomes randomly oriented, and the population of RD12 on the edge-on arrangement increases. By adding the rubbed PI coated substrate, the interactions between RD12 mesogens and the PI surface are significantly increased, and the N → K_{T1} phase transition is greatly depressed. This phenomenon can be explained by the cooperative anchoring interaction. By rubbing the PI layer, the long axes of rod and disc mesogens of RD12 on the planar alignment layer are parallel to the rubbing direction and create a monodomain in the cell. Note that the whole shape of RD12 on the PI coated/rubbed substrate is ribbonlike. Since the phase-on arrangement of RD12 on the surface is continuously and cooperatively transferred into the middle of the cell along the cell thickness direction, the whole RD12 molecules in the LC cell can cooperatively retain the N phase and delay the N → K_{T1} phase transition in particular when the cell thickness is small. By increasing the cell thickness, this cooperation in the middle of the cell thickness direction becomes weaker, and the phase transition behavior gradually approaches that in the bulk, as schematically illustrated in Figure 6c–e. After the K_{T2} and K_{T1} crystallization in the LC cell, the interactions created

dx.doi.org/10.1021/cg301777y | Cryst. Growth Des. 2013, 13, 1309–1315

among RD12 molecules in three dimensions is much stronger than the anchoring interactions between RD12 and the substrate so that the $K_{T2} \rightarrow K_{T1}$ and $K_{T1} \rightarrow N$ phase transitions are fairly independent of the surface chemistry and physics as well as the cell thickness.

Metastability of a Glassy Nematic Phase via the Competition between Surface Anchoring and Crystallization Forces. To understand the thermodynamic phase transition behaviors of RD12 and the formation of the K_{T2} metastable crystalline phase,[56,57] the free energy versus temperature at constant pressure is schematically illustrated in Figure 7. As represented as blue arrows in Figure 7a, upon cooling the bulk RD12 of which there is no strong surface anchoring interactions, the I phase transfers to the N phase which possesses the lowest free energy phase between T_{NI} and T_{KT1N}. The continuous slow cooling (1 °C/min) allows the $N \rightarrow K_{T1}$ phase transition in which the K_{T1} phase shows the lowest free energy. The subsequent heating leads to the $K_{T1} \rightarrow N \rightarrow I$ phase transitions, as illustrated in Figure 7a. When the PI coated/rubbed LC cell with d = 4.4 μm is slowly cooled at 1 °C/min, the I phase transfers to the N phase at T_{NI}, which is identical to the case in the bulk. However, the N phase formed in the PI coated/rubbed LC cell with d = 4.4 μm bypasses the K_{T1} and K_{T2} crystalline phases at this cooling rate and retains the N phase until the temperature reaches T_g to form the glassy N phase (the cooling track is represented as blue arrows). The glassy N phase also can be formed by quickly quenching the bulk RD12 to a temperature below the T_g. Therefore, it can be considered that the surface anchoring interaction dominates the transition behavior of forming crystalline phase from the N phase when the rubbed PI alignment layer is introduced. Note that the free energy of the K_{T1} is lower than that of the K_{T2} in the whole temperature range studied. Therefore, the K_{T2} crystalline phase is metastable compared with the K_{T1} crystalline phase. The subsequent heating of the glassy N phase to above the T_g undergoes the pathway to a lower free energy state of the metastable K_{T2} crystalline phase first, and then the K_{T2} transfers to the stable K_{T1} crystalline phase at a higher temperature. The stable K_{T1} crystalline phase transfers to the N phase at T_{KT1N} and to the I phase at T_{NI}. As experimentally observed (Figure 4), the phase transition temperatures of the $K_{T1} \rightarrow N$ and the $N \rightarrow I$ are independent of the surface anchoring interactions and identical to those in the bulk RD12.

On the basis of the schematic illustration in Figure 7b, the phase transition temperatures of the glassy $N \rightarrow K_{T2}$ and the $K_{T2} \rightarrow K_{T1}$ depend on the heating rates and surface anchoring interactions. A slower heating rate and a lower surface anchoring interaction will decrease the phase transition temperatures of the glassy $N \rightarrow K_{T2}$ and the $K_{T2} \rightarrow K_{T1}$. To support this explanation, the PI coated/rubbed LC cells with d = 4.4 μm is prepared by cooling at 1 °C/min, and then it is annealed at 25 °C. At least for three months, there is no indication that the glassy $N \rightarrow K_{T2}$ phase transition has taken place. This is because the cooperative translational motions of RD12 molecules are not possible below the T_g = 38 °C. Phase transition behaviors of RD12 during the annealing process at 50 °C are also monitored, and the results are summarized in Figure 8. The metastable K_{T2} crystalline phase starts to emerge against the glassy N background after 150 min at 50 °C, and this metastable K_{T2} crystalline phase then transfers to the stable K_{T1} crystalline phase after 1400 min at 50 °C. This transition sequence clearly provides the evidence for explaining the thermodynamic phase transition behaviors of RD12 and the formation of the K_{T2} metastable crystalline phase (Figure 7).

CONCLUSIONS

Surface-induced phase evolutions of a rod-disc LC molecule (RD12) were investigated by varying the surface chemistry and physics. Upon varying the LC cell thickness and their surface chemical and physical environments, the RD12 phase transition behaviors were dramatically changed compared with those in the bulk. It was found that the N phase of RD12 in the PI coated/rubbed LC cell with d = 4.4 μm effectively expanded its stability in a wide temperature region between the isotropization and glass transition temperature, and the crystallization of RD12 was completely suppressed. Since the phase-on arrangement of RD12 on the surface can be continuously and cooperatively transferred into the middle of the cell along the cell thickness direction, the whole RD12 molecules in the LC cell can cooperatively retain the N phase and delay the $N \rightarrow K_{T1}$ phase transition. On the basis of our careful experimental results, we concluded that the formation of the glassy N phase was mainly because the surface anchoring interactions can overcome the physical interactions of RD12 themselves by the introduction of the rubbed PI alignment layer in particular when the cell thickness is small. After the complete transformation from the metastable K_{T1} crystalline phase to the stable K_{T1} phase, the thermodynamic phase transitions at the higher temperature were independent of the surface anchoring interactions. The tailored molecular alignment and anisotropic physical properties of the glassy N phase of RD12 can allow us to fabricate smart optical and electrical thin films for practical applications in electro-optical uses.

AUTHOR INFORMATION

Corresponding Author

*Fax: 82 63 270 2341. Tel: +82 63 270 4633. E-mail: kujeong@jbnu.ac.kr (K.-U.J.); lsh1@chonbuk.ac.kr (S. H. L.).

Author Contributions

#These authors contributed equally to this work.

Notes

The authors declare no competing financial interest.

ACKNOWLEDGMENTS

This work was mainly supported by Converging Research Center Program (2012K001428), World Class University Program (R31-20029), and Human Resource Training Project for Regional Innovation funded by the Ministry of Education, Science, and Technology of Korea.

REFERENCES

(1) Kelker, H.; Knoll, P. M. *Liq. Cryst.* **1989**, *5*, 19.
(2) Lehmann, O. Z. *Phys. Chem.* **1888**, *9*, 421.
(3) Tamman, G. *Ann. Phys.* **1901**, *3*, 524.
(4) Schadt, M.; Buchecker, R.; Mueller, K. *Liq. Cryst.* **1989**, *5*, 293.
(5) Lee, S. H.; Lee, S. L.; Kim, H. Y.; Eom, T. Y. *J. Korean Phys. Soc.* **1999**, *35*, 1111.
(6) Wang, P.; Moorefield, C. N.; Jeong, K.-U.; Hwang, S.-H.; Li, S.; Cheng, S. Z. D.; Newkome, G. R. *Adv. Mater.* **2008**, *20*, 1381.
(7) Xue, C.; Jin, S.; Weng, X.; Ge, J. J.; Shen, Z.; Shen, H.; Graham, M. J.; Jeong, K.-U.; Huang, H.; Zhang, D.; Guo, M.; Harris, F. W.; Cheng, S. Z. D. *Chem. Mater.* **2004**, *16*, 1014.
(8) Ye, C.; Xu, G.; Yu, Z.-Q.; Lam, J. W. Y.; Jang, J. H.; Peng, H.-L.; Tu, Y.-F.; Liu, Z.-F.; Jeong, K.-U.; Cheng, S. Z. D.; Chen, E.-Q.; Tang, B. Z. *J. Am. Chem. Soc.* **2005**, *127*, 7668.

(9) Jeong, K.-U.; Knapp, B. S.; Ge, J. J.; Graham, M. J.; Tu, Y.; Leng, S.; Xiong, H.; Harris, F. W.; Cheng, S. Z. D. *Polymer* **2006**, *47*, 3351.
(10) Ruan, J.-J.; Jin, S.; Ge, J. J.; Jeong, K.-U.; Graham, M. J.; Zhang, D.; Harris, F. W.; Lotz, B.; Cheng, S. Z. D. *Polymer* **2006**, *47*, 4182.
(11) Jing, S.; Jeong, K.-U.; Tu, Y.; Graham, M. J.; Wang, J.; Harris, F. W.; Cheng, S. Z. D. *Macromoleules* **2007**, *40*, 5450.
(12) Wang, L.; Jeong, K.-U.; Lee, M.-H. *J. Mater. Chem.* **2008**, *18*, 2657.
(13) Choi, H. J.; Jeong, K.-U.; Chien, L.-C.; Lee, M.-H. *J. Mater. Chem.* **2009**, *19*, 7124.
(14) Bae, Y.-J.; Yang, H.-J.; Shin, S.-H.; Jeong, K.-U.; Lee, M.-H. *J. Mater. Chem.* **2011**, *21*, 2074.
(15) Wang, L.; Cho, H.; Lee, S.-H.; Lee, C.; Jeong, K.-U.; Lee, M.-H. *J. Mater. Chem.* **2011**, *21*, 60.
(16) Park, S. W.; Lim, S. H.; Choi, Y. E.; Jeong, K.-U.; Lee, M.-H.; Chang, H. S.; Kim, H. S.; Lee, S. H. *Liq. Cryst.* **2012**, *39*, 501.
(17) Kim, D.-Y.; Wang, L.; Cao, Y.; Yu, X.; Cheng, S. Z. D.; Kuo, S.-W.; Song, D.-H.; Lee, S. H.; Lee, M.-H.; Jeong, K.-U. *J. Mater. Chem.* **2012**, *22*, 17382.
(18) Kim, S.; Kang, S.-W.; Jeong, K.-U. *Soft Matter* **2012**, *8*, 9761.
(19) Kim, N.; Wang, L.; Kim, D.-Y.; Hwang, S.-H.; Kuo, S.-W.; Lee, M.-H.; Jeong, K.-U. *Soft Matter* **2012**, *8*, 9183.
(20) Goodby, J. W.; Waugh, M. A.; Stein, S. M.; Chin, E.; Pindak, R.; Patel, J. S. *Nature* **1989**, *337*, 449.
(21) Goodby, J. W.; Waugh, M. A.; Stein, S. M.; Chin, E.; Pindak, R.; Patel, J. S. *J. Am. Chem. Soc.* **1989**, *111*, 8119.
(22) Goodby, J. W. *Curr. Opin. Colloid Interface Sci.* **2002**, *7*, 326.
(23) Kikuchi, H.; Yokota, M.; Hisakado, Y.; Yang, H.; Kajiyama, T. *Nat. Mater.* **2002**, *1*, 64.
(24) Lee, M.; Hur, S.-T.; Higuchi, H.; Song, K.; Choi, S.-W.; Kikuchi, H. *J. Mater. Chem.* **2010**, *20*, 5813.
(25) Castles, F.; Morris, S. M.; Terentjev, E. M.; Coles, H. *J. Phys. Rev. Lett.* **2010**, *104*, 157801.
(26) Pelzl, G.; Diele, S.; Weissflog, W. *Adv. Mater.* **1999**, *11*, 707.
(27) Link, D. R.; Natale, G.; Shao, R.; McLennan, J. E.; Clark, N. A.; Korblova, E.; Walba, D. M. *Science* **1997**, *278*, 1924.
(28) Jeong, K.-U.; Yang, D.-K.; Graham, M.-J.; Tu, Y.; Kuo, S.-W.; Knapp, B. S.; Harris, F. W.; Cheng, S. Z. D. *Adv. Mater.* **2006**, *18*, 3229.
(29) Jeong, K.-U.; Knapp, B. S.; Ge, J. J.; Jin, S.; Graham, M. J.; Xiong, H.; Harris, F. W.; Cheng, S. Z. D. *Macromolecules* **2005**, *38*, 8333.
(30) Jeong, K.-U.; Knapp, B. S.; Ge, J. J.; Jin, S.; Graham, M. J.; Harris, F. W.; Cheng, S. Z. D. *Chem. Mater.* **2006**, *18*, 680.
(31) Madsen, L. A.; Dingemans, T. J.; Nakata, M.; Samulski, E. T. *Phys. Rev. Lett.* **2004**, *92*, 145505.
(32) Yu, L. J; Saupe, A. *Phys. Rev. Lett.* **1980**, *45*, 1000.
(33) Jeong, K.-U.; Jin, S.; Ge, J. J.; Knapp, B. S.; Graham, M. J.; Ruan, J.; Guo, M.; Xiong, H.; Harris, F. W.; Cheng, S. Z. D. *Chem. Mater.* **2005**, *17*, 2852.
(34) Lee, S. H.; Bhattacharyya, S. S.; Jin, H. S.; Jeong, K.-U. *J. Mater. Chem.* **2012**, *22*, 11893.
(35) Semenza, P. *Inf. Disp.* **2009**, *25*, 22.
(36) Lee, S. H.; Hong, S. H.; Kim, J. M.; Kim, H. Y.; Lee, J. Y. *J. Soc. Inf. Disp.* **2001**, *9*, 155.
(37) Jeong, K.-U.; Jing, A. J.; Monsdorf, B.; Graham, M. J.; Harris, F. W.; Cheng, S. Z. D. *J. Phys. Chem. B* **2007**, *111*, 767.
(38) Jeong, K.-U.; Jing, A. J.; Mansdorf, B.; Graham, M. J.; Yang, D.-K.; Harris, F. W.; Cheng, S. Z. D. *Chem. Mater.* **2007**, *19*, 2921.
(39) Mansdorf, B. Ph.D. Dissertation, University of Akron, 2003.
(40) Jeong, K.-U.; Jing, A. J.; Mansdorf, B.; Graham, M. J.; Tu, Y.; Harris, F. W.; Cheng, S. Z. D. *Chin. J. Polym. Sci.* **2007**, *25*, 57.
(41) Jung, J. H.; Kim, S.-E.; Song, E. K.; Ha, K. S.; Kim, N.; Cao, Y.; Tsai, C.-C.; Cheng, S. Z. D.; Lee, S. H.; Jeong, K.-U. *Chem. Mater.* **2010**, *22*, 4798.
(42) Schiekel, M. F.; Fahrenschon, K. *Appl. Phys. Lett.* **1971**, *19*, 391.
(43) Soref, R. A.; Rafuse, M. J. *J. Appl. Phys.* **1972**, *43*, 2029.
(44) Ong, H. L. *Appl. Phys. Lett.* **1991**, *59*, 155.
(45) Wu, S. *Polymer Interface and Adhesion*; Dekker: New York, 1982.
(46) van Oss, C. J. *Interfacial Forces in Aqueous Media*; Dekker: New York, 1994.
(47) Owens, D. K.; Wendt, R. C. *J. Appl. Polym. Sci.* **1969**, *13*, 1741.
(48) Chandran, S. P.; Mondiot, F.; Mondain-Monval, O.; Loudet, J. C. *Langmuir* **2011**, *27*, 15185.
(49) Ruths, M.; Zappone, B. *Langmuir* **2012**, *28*, 8371.
(50) Zhou, J.; Collard, D. M.; Park, J. O.; Srinivasarao, M. *J. Am. Chem. Soc.* **2002**, *124*, 9980.
(51) Zhou, J.; Collard, D. M.; Park, J. O.; Srinivasarao, M. *J. Phys. Chem. B* **2005**, *109*, 8838.
(52) Noonan, P. S.; Shavit, A.; Acharya, B. R.; Schwartz, D. K. *ACS. Appl. Mater. Interfaces* **2011**, *3*, 4374.
(53) Lockwood, N. A.; de Pablo, J. J.; Abbott, N. L. *Langmuir* **2005**, *21*, 6805.
(54) Kim, Y. H.; Yoon, D. K.; Jeong, H. S.; Lavrentovich, O. D.; Jung, H.-T. *Adv. Funct. Mater.* **2011**, *21*, 610.
(55) Ryschenkow, G.; Kleman, M. *J. Chem. Phys.* **1976**, *64*, 404.
(56) Keller, A.; Cheng, S. Z. D. *Polymer* **1998**, *39*, 4461.
(57) Cheng, S. Z. D. *Phase Transitions in Polymers: The Role of Metastable States*; Elsevier: New York, 2008.